Survey of jointed rock mass from 3D point clouds for the wedge stability analysis

A. Menéndez-Díaz[(a)], C. Ordóñez-Galán [(b)], JB. Bouza-Rodríguez [(c)], S. García-Cortés [(b)]

[(a)] Department of Manufacturing Engineering, Universidad de Oviedo.
[(b)] Department of Mining Engineering, Universidad de Oviedo.
[(c)] Escuela de Ingeniería Industrial, Universidad de Vigo.

Article Information

Keywords:
3D point cloud,
key block,
clustering,
photogrammetry,
TLS.

Corresponding author:
A. Menéndez-Díaz
Tel.: 985 104244
Fax.: 985 104242
e-mail: amenendez@uniovi.es
Address: ETS Ingenieros de Minas, Independencia, 13, 33004, Oviedo, Spain.

Abstract

Measurement of discontinuities in jointed rock masses by direct methods – using compasses and tapes – is sometimes complex, laborious and dangerous, especially in high and steep slopes. Under these conditions it can be necessary to hire professional climbers or, in worst situations, it becomes definitely impossible to take measurements. An alternative to direct methods are indirect methods such as photogrammetry or terrestrial laser scanning (TLS).

We present an approach for automatic detection of discontinuities in jointed rock masses from a 3D point cloud. It consists on a sequence of processes for feature extraction and characterization of the discontinuities that use voxelization, robust detection of planes by sequential RANSAC and clustering.

The results obtained by applying this methodology to the 3D point cloud are a set of discontinuity families, characterized by their dips and dip directions, and surface wedges. The ultimate goal is the stability analysis of the mass rock using the limit equilibrium method.

1 Introduction

Discontinuities divide a rock mass into blocks of different shapes and sizes. When an excavation is made in a rock mass, new different-sized blocks with irregular faces – called 'key blocks' [1,2,3] – are formed, which may detach, overturn or slide, potentially compromising the stability of the excavation and possibly causing accidents.

The classic method for characterizing a rock mass is to measure discontinuity position, orientation, dip, size and spacing using a compass, a clinometer and a ruler. A major limitation to this approach is accessing discontinuities – often inaccessible, for instance, in large vertical slopes, when professional climbers need to be used. Data collection, furthermore, is restricted to a few specific points on the solid rock mass. Considerable time is generally invested in acquiring the information necessary to characterize a rock mass, so an alternative is to use some method that does not require direct contact with the rock mass, for instance, terrestrial photogrammetry and terrestrial laser scanning [4, 5].

Terrestrial photogrammetry creates, from a set of images, a digital terrain model in which discontinuities can be identified in order to characterize a rock mass [6,7,8]. They used close-range photogrammetry to obtain rock mass images from which to determine, using a multi-resolution random sample consensus (RANSAC) algorithm, the location and orientation of discontinuity planes.

Terrestrial laser scanning (TLS) obtains fast and accurate 3D models of objects as clouds of points, thereby creating a permanent record in the moment of measurement and permitting great flexibility during data processing. TLS has, in recent years, acquired popularity as an approach to geometrically analysing large surfaces [9]. For the particular case of fractured rock masses, TLS point clouds can be used to identify discontinuity planes, determine the geometric characteristics of joints (position, orientation, dip, etc) and calculate the volume of potentially unstable blocks [10,11].

Key blocks were initially studied using vector geometry [12]; subsequently topological techniques were developed to identify the features of complex blocks [13,14]. Shi and Goodman [15] performed a detailed study of the stability of blocks, determining removable blocks according to the free faces of the excavation and sliding directions according to the active forces. Mauldon and Goodman [16] developed this method further to account for rotational movements. Probabilistic block analyses have also been made by several researchers [17,18]. This approach takes into account variations in discontinuity characteristics and calculates probabilities for block shapes and sizes and their stability.

The default stability analysis is the key block method (KBM), which is based on the assumption that certain blocks are subject to gravitational loading only and the instabilities are associated with local phenomena of collapsing blocks, where using the limit equilibrium method makes sense.

We studied potentially unstable blocks in a tunnel excavated in a rock mass that was originally used to transport coal but is now scheduled for development as part of a tourist route. Geometric information on the discontinuity sets in the rock mass was obtained from a point cloud obtained via TLS and a stability analysis was

performed using the KBM considering both pyramidal and non-pyramidal blocks.

2 Methodology

2.1 Data acquisition of jointed mass rock

The detection of rock discontinuities from 3D point clouds can be done manually, semi-automatically or automatically. Manual scanning is usually done using images superimposed on the point cloud, with a qualified expert drawing the discontinuity planes. In semi-automatic detection an expert decides the location of the discontinuity planes but uses fitting algorithms as an alternative to drawing the planes. Automatic detection can be understood as a segmentation problem. From this point of view, growing or aggregation algorithms can be used to solve the problem. Growing algorithms are more easily implemented and more rapidly executed but have several drawbacks in relation to seed selection and discontinuities [2]. Aggregation methods are slower but are more appropriate for densely featured spaces such as those obtained for rock discontinuities. We tested both semi-automatic and automatic methods for detecting discontinuity planes.

Automatic detection consists of three stages: voxelization, plane extraction and clustering (see fig 1)

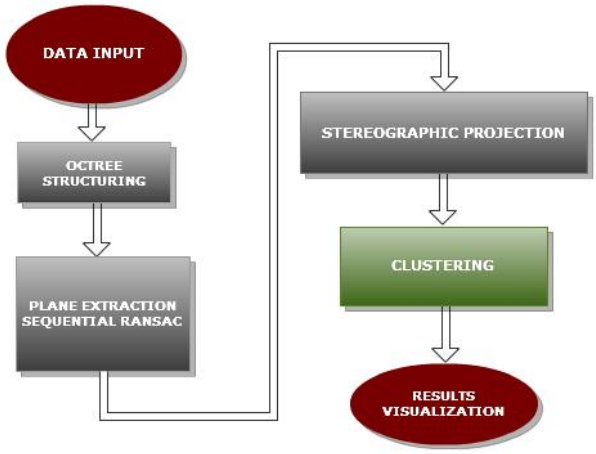

Fig. 1 Global procedure flowchart.

1) Voxelization. The process of detecting discontinuities is launched by voxelizing the point cloud defining the rock mass. Due to the constant resolution of the point cloud all the voxels were of the same size. Voxel size was determined based on the mean point density. Each voxel stored basic information such as indexes for the contained points, gravity centre coordinates, voxel size and normal vectors for the extracted planes if applicable.

2) Plane extraction. The objective of plane extraction is to identify all the planes on the rock surface covered by the point cloud. An adaptive RANSAC method [20] was used for this purpose. A minimum number of four points was required for any plane to be extracted. The inliers points for each extracted plane were removed from the point cloud in each run. A least squares plane fitting the inliers was calculated in order to improve the quality of the detection. The procedure was repeated three times for each voxel in order to extract a maximum of three planes. If voxel size was reasonably small, this number of planes was estimated to be enough to model the rock surface inside the voxel. Other standard modifications were implemented in the RANSAC procedure, including the use of standard deviations for the inlier mean distances to the plane, the cardinality of the consensus set [21] and adaptive estimates of the number of iterations while locating the inliers [8].

3) Clustering. Once the discontinuity planes were determined, their normal vectors were represented as points over a stereographic net. A clustering fuzzy k-means algorithm then detected the different sets of planes. An analysis of the orientation of the three intersecting planes identified wedges on the surface of the rock mass. No plane aggregation procedure was implemented, since aggregation tends to smooth discontinuity directions and eliminate statistical information on dip angles and directions.

Semi-automatic detection is a simplification of automatic detection, with discontinuities detected visually from the point cloud, preferably using superimposed photographs. Equations are automatically extracted for the planes that best fit these points from the least squares point of view. As with automatic detection, the direction and dip of the joint sets in the rock mass are determined from these planes using stereographic projection.

2.2 Stability of key block method

The stability of key blocks need to be investigated in order to design and plan support for an excavation. The KBM is based on analysing the distribution of the various blocks along discontinuity surfaces and determining the conditions in which these blocks lose their kinematic stability. The KBM can be implemented using one of the following stability analysis methods:

We used a ubiquitous approach, applying a series of simplifying assumptions:

1) All the joint surfaces are perfectly planar.
2) Joint surfaces extend entirely through the rock mass.
3) Blocks defined by the system of joint faces are rigid.
4) Limit equilibrium analysis is applied.

Fig 2 shows the different types of pyramidal and non-pyramidal blocks that can be formed [19]. Tetrahedral pyramidal blocks are formed by three sets of planes (Type I); when four planes not contained in the free face go through a vertex, pentahedral pyramidal blocks are formed (Type II-a), and when these planes intersect at an edge, pentahedral non-pyramidal blocks are formed (Type II-b).

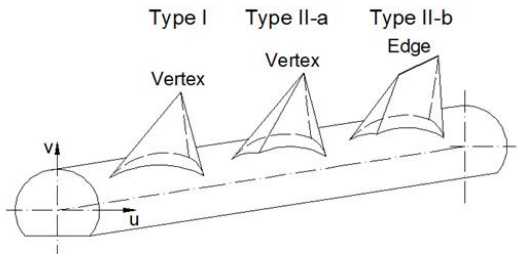

Fig. 2 Types of keyblocks.

The KBLOCK program analysed the kinematic stability of these blocks to break off in each tunnel section and identified the combination of discontinuity sets that generated critical blocks in the tunnel crown and walls. KBLOCK is implemented in C++ using the OpenGL library.

3 Application

3.1 Study area and joint survey

The methodology was applied to the stability analysis of a tunnel in the Riosa (Asturias, NW Spain). The tunnel is now unused, but a tourist trail is planned for the area that will include the tunnel (fig 3); this is why a study of the stability of the tunnel is necessary.

Fig. 3 Old railway tunnel and jointed rock mass in the area

For geometric characterization of the rock mass discontinuities we used a RIEGL® LMS-Z390i time-of-flight scanner, with a range above 400 m for objects with reflectance greater than 80%, 6 mm accuracy for a single point and a data capture rate of 8000 data points/second. Coupled to the top was a Nikon D90 digital SLR camera calibrated to apply false colour to the 3D model and so facilitate the identification of areas with discontinuities (see fig 4).

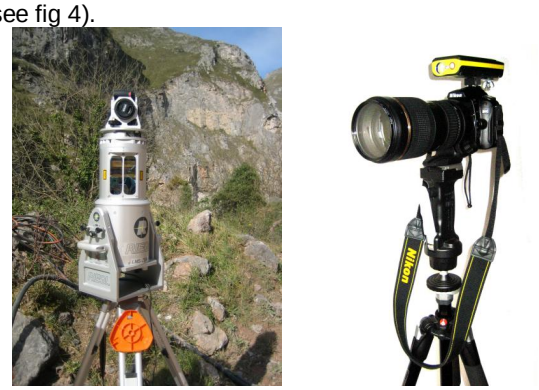

Fig. 4 RIEGL LMS-Z390i scaner and the calibrated camara Nikon D90

Scanning density was 0.25 points/cm2, for a distance to the rock mass of between 10 m and 15 m, resulting in a point cloud of approximately 1.4 million points. This cloud was treated with an application of colour from photographs taken with the ShapeMetrix3D software.

In the following, only a part of the outcrop over the tunnel mouth is processed. The algorithm implemented allows the user to introduce the following parameters:

- Average point number in each voxel.
- Plane support inside a voxel as a percentage.
- Point to plane distance tolerance.
- Number of repetitions in the clustering algorithm.

The discontinuities were detected using the automatic and semi-automatic methods described above. Fig 5 shows the planes determined by the automatic method within each voxel in the top part of the tunnel.

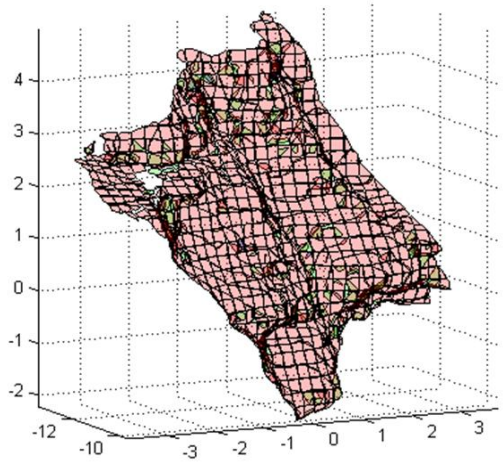

Fig. 5 Discretization in voxels and joint planes detected by the automatic method based on sequential RANSAC.

Overall the semi-automatic method is preferred by experts, although the automatic system detects discontinuity sets that technicians sometimes fail to recognize in the point cloud. Fig 6 shows, for the point cloud obtained with the laser scanner with colour information provided by the camera, the main sets of joints detected.

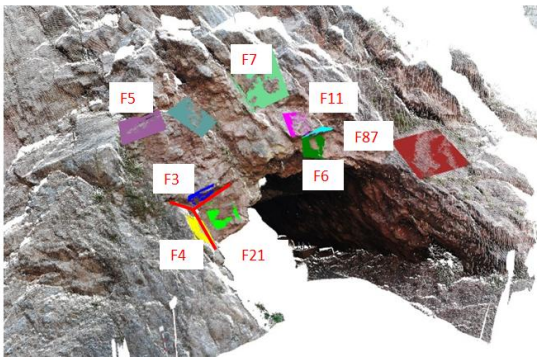

Fig. 6 3D point cloud and joints detected

Fig 7 lists the parameters for the main sets of joints. To the right is the stereographic projection of the poles for each discontinuity sets.

Joint Set	Dip Direction α_i	Dip β_i	Spacing
F1	242º	88º	2.0 m
F2	81º	59º	0.5 m
F3	232º	44º	0.5 m
F4	358º	62º	0.8 m
F5	71º	63º	0.8 m
F6	61º	60º	1.2 m
F7	63º	75º	0.4 m
F8	256º	28º	1.0 m

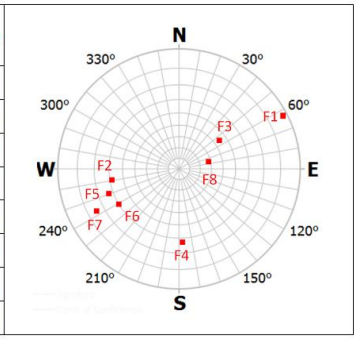

Fig. 7 Joint sets identified in the point cloud

3.2 Stability analysis

The stability analysis focused on a stretch of 30 metres of tunnel running in a north-westerly direction with a trend of 35º and a plunge of 3º.

The parameter values assigned to each discontinuity (tab 1) were included with the values shown in Tab 1.

Joint set	Spacing	Cohesion	Friction angle	Tensile strength
F1	2.0 m	10.0 kPa	10º	1.0 kPa
F2	0.5 m	10.0 kPa	10º	1.0 kPa
F3	0.5 m	50 kPa	35º	5 kPa
F4	0.8 m	100 kPa	25º	10 kPa
F5	0.8 m	10.0 kPa	10º	1.0 kPa
F6	1.2 m	100 kPa	35º	10 kPa
F7	0.4 m	10.0 kPa	10º	1.0 kPa
F8	1.0 m	100 kPa	35º	10 kPa

Tab. 1 Values of the rock mass joint sets.

To determine these values the area was geologically surveyed and materials forming discontinuities were sampled and shear-tested. The rock mass around the tunnel consists of Palaeozoic materials (mountain limestone) formed of micrites, microsporites and dolomicrites, with stratification ranging from massive to pleated, and predominantly dark grey to black in colour and foetid. The limestone is altered locally with a significant presence of dolomite rock. Periodic explosions and extraction activities carried out in the nearby quarry has reduced rock mass strength, increased fracturing and facilitated weathering.

Tab 2 lists all the safety factors using KBLOCK; specified are 56 combinations of discontinuity sets that generate removable pyramidal blocks. Indicated in the first three columns for each combination are the sets that form the combination and the removable blocks formed by these three sets. At most a combination of three planes could form different blocks (BO1, BO2, BO3, B04); however, the position of the gallery made it only possible to remove the blocks indicated by the red or green boxes, representing unstable blocks (with a safety factor below 1.3) and stable blocks (with the corresponding safety factor), respectively.

Combination	Joint Set			Block			
C	1	2	3	B01	B02	B03	B04
1	F1	F2	F3	2.30	4.25		
2	F1	F2	F4	49.54	0.34	27.49	11.26
3	F1	F3	F4	3.05	7.81	28.10	2.07
4	F2	F3	F4	27.18	19.77	22.36	0.72
5	F1	F2	F5	1.59	1.35		
6	F1	F3	F5	4.15			
7	F2	F3	F5	1.63	28.15		
8	F1	F4	F5	17.38	0.54		
9	F2	F4	F5	1.53	4.17	22.58	
10	F3	F4	F5	13.07	24.50	0.95	31.26
11	F1	F2	F6	28.02	2.90		
12	F1	F3	F6	17.35			
13	F2	F3	F6	1.56	5.26		
14	F1	F4	F6	7.94	16.72	1.76	
15	F2	F4	F6	9.24			
16	F3	F4	F6	26.16	1.18	46.67	
17	F1	F5	F6	5.43			
18	F2	F5	F6	41.84	3.13		
19	F3	F5	F6	4.05	11.43		
20	F4	F5	F6	11.31			
21	F1	F2	F7	0.98	0.62		
22	F1	F3	F7	3.15			
23	F2	F3	F7	0.85	30.92	12.77	
24	F1	F4	F7	18.51	1.09		
25	F2	F4	F7	1.09	23.83	11.68	
26	F3	F4	F7	9.29	30.54	1.22	43.40
27	F1	F5	F7	1.22	1.05		
28	F2	F5	F7	3.03			
29	F3	F5	F7	1.11	18.94		
30	F4	F5	F7	2.23	23.13	34.13	
31	F1	F6	F7	45.33			
32	F2	F6	F7	6.66	6.01		
33	F3	F6	F7	21.08			
34	F4	F6	F7	25.60	9.96	29.39	
35	F5	F6	F7	20.16	27.26	18.15	
36	F1	F2	F8	41.51	2.39	3.71	
37	F1	F3	F8	28.26			
38	F2	F3	F8	30.81	6.76	30.45	13.37
39	F1	F4	F8	22.11	4.67	2.59	
40	F2	F4	F8	18.92			
41	F3	F4	F8	8.27			
42	F1	F5	F8	37.45	4.37	4.00	
43	F2	F5	F8	12.93	4.12		
44	F3	F5	F8	25.28	18.91	7.90	
45	F4	F5	F8	4.82	5.70	13.26	
46	F1	F6	F8	7.12			
47	F2	F6	F8	25.12	19.73		
48	F3	F6	F8	25.24			
49	F4	F6	F8	7.81	6.23	15.69	
50	F5	F6	F8	27.73			
51	F1	F7	F8	34.91	32.56		
52	F2	F7	F8	12.99	2.44		
53	F3	F7	F8	27.63	28.84		
54	F4	F7	F8	8.58	5.03	7.77	
55	F5	F7	F8	11.30	4.55		
56	F6	F7	F8	10.03			

Tab. 2 Safety factors key-block of type I.

For instance the unstable crown block, formed by the F1, F2 and F4 sets, have a safety factor of 0.34, volume of 1.18 m3 and weight of 2.61 tonnes. In the right wall the keyblock is much smaller, with a safety factor of 3.98 and a maximum volume of 0.02 m3. Blocks are also formed between the floor and the left sidewall, but these are typically stable.

The left sidewall was the most unstable, with lower safety factors for its blocks, as illustrated in fig 8, which shows the orthographic projection for the non-pyramidal pentahedral block formed by the F2, F3, F5, F7 discontinuity sets. This unstable block had a safety factor of 0.81 and weighed 62 tonnes.

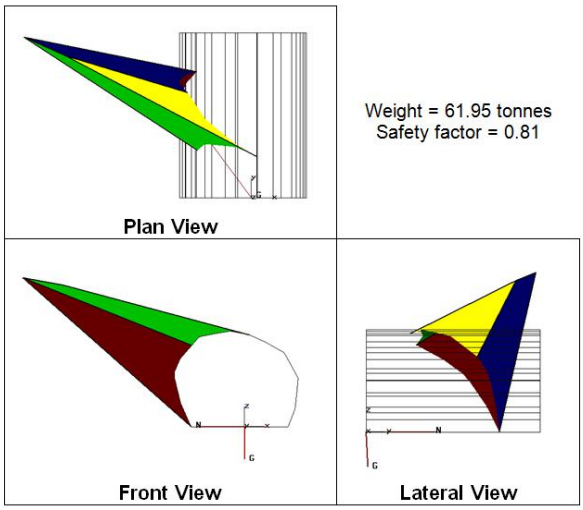

Fig. 8 Orthographic projections for the block formed by the joints F2, F3, F5 and F7 .

4 Conclusion

In the automatic methods for detecting discontinuity planes, point to plane distance tolerance seems to be a more sensitive parameter affecting the results. Rock masses hardly show perfect planes over their surfaces so this suggests the use of low values for this factor. However, if the tolerance is very large, the detection of three different planes inside each voxel is not achieved reducing the capability of wedge detection. To deal with these aspects we plan to implement some other robust approaches like Hough 3D [21] that can also perform plane extraction but in addition it can supply some information pertaining to the number of planes present in each voxel.

Semi-automatic detection is a simplification of automatic detection, with joints detected visually by the geologist from the point cloud, using superimposed photographs. This improve the data quality of the joints sets thanks to the knowledge of the geologist.

Overall the semi-automatic method is preferred by experts, although the automatic system detects discontinuity sets that technicians sometimes fail to recognize in the point cloud.

For the tunnel in this study, the best solution would be preventive bolting in the left sidewall to ensure stability. This would increase the shear forces between adjacent blocks and, in turn, the frictional forces, thereby increasing the safety factor of the blocks in this sidewall.

Acknowledgement

This paper has been funded by the Government of the Principality of Asturias through funds from the Programme of Science, Technology and Innovation (PCTI), co-financed by Operational Programme FEDER of the Principality of Asturias 2007-2013 (Research project FC-11-PC10-08), and the Project BIA2011-26915 of the Spanish Ministry of Science and Innovation.

References

[1] Wang, S.H., et al. *3-D stability analysis of tunnel structures based on geometric stochastic blocks theory*. 2008. Beijing.

[2] Fekete, S., M. Diederichs, and M. Lato, *Geotechnical and operational applications for 3-dimensional laser scanning in drill and blast tunnels*. Tunnelling and Underground Space Technology, 2010. 25(5): p. 614-628.

[3] Ferrero, A.M., et al. *Development of a non-contact survey method of tunnel excavation face for DEM modelling*. 2012. Beijing

[4] Donovan, J. and A. Lebaron. *A comparison of photogrammetry and laser scanning for the purpose of automated rock mass characterization*. 2009. Asheville, NC.

[5] Ferrero, A.M., et al., *Advanced geostructural survey methods applied to rock mass characterization*. Rock Mechanics and Rock Engineering, 2009. 42(4): p. 631-665

[6] Rogers, S.F., et al. *Characterising the in situ fragmentation of a fractured rock mass using a discrete fracture network approach*. 2007. Vancouver, BC

[7] Wang, F., et al., *Study on geometrical information of obtaining rock mass discontinuities based on VirtuoZo*. Yanshilixue Yu Gongcheng Xuebao/Chinese Journal of Rock Mechanics and Engineering, 2008. 27(1): p. 169-175.

[8] Roncella, R., G. Forlani, and F. Remondino. *Photogrammetry for geological applications: Automatic retrieval of discontinuity orientation in rock slopes*. 2005. San Jose, CA.

[9] Armesto, J., et al., *Terrestrial laser scanning used to determine the geometry of a granite boulder for stability analysis purposes. Geomorphology*, 2009. 106(3-4): p. 271-277.

[10] Lato, M.J., et al., *Evaluating roadside rockmasses for rockfall hazards using LiDAR data: Optimizing data collection and processing protocols.* Natural Hazards, 2012. 60(3): p. 831-864.

[11] Ferrero, A.M., et al., *Rock slopes risk assessment based on advanced geostructural survey techniques*. Landslides, 2011. 8(2): p. 221-231.

[12] Warburton, P.M., *Vector stability analysis of an arbitrary polyhedral rock block with any number of free faces*. International Journal of Rock Mechanics and Mining Sciences and, 1981. 18(5): p. 415-427.

[13] Jing, L., *Block system construction for three-dimensional discrete element models of fractured rocks*. International Journal of Rock Mechanics and Mining Sciences, 2000. 37(4**):** p. 645-659.

[14] Lu, J., *Systematic identification of polyhedral rock blocks with arbitrary joints and faults*. Computers and Geotechnics, 2002. 29(1): p. 49-72.

[15] Goodman, R.E. and G.H. Shi, Block theory and its application to rock engineering. Block Theory and Its Application to Rock Engineering, 1985.

[16] Mauldon, M.G., RE, *Vector analysis of key block rotations*. Journal of Geotechnical Engineering, 1996. 109-122: p. 976-987.
[17] Park, H. and T.R. West, *Development of a probabilistic approach for rock wedge failure*. Engineering Geology, 2001. 59(3-4): p. 233-251.
[18] Yarahmadi Bafghi, A.R. and T. Verdel, *The probabilistic key-group method*. International Journal for Numerical and Analytical Methods in Geomechanics, 2004. 28(9): p. 899-917.
[19] Menéndez-Díaz, A., et al., *Analysis of tetrahedral and pentahedral key blocks in underground excavations*. Computers and Geotechnics, 2009. 36(6): p. 1009-1023.
[20] Sturzenegger, M. and D. Stead, *Quantifying discontinuity orientation and persistence on high mountain rock slopes and large landslides using terrestrial remote sensing techniques*. Natural Hazards and Earth System Science, 2009. 9(2): p. 267-287.
[21] Tarsha-Kurdi, F., T. Landes, and P. Grussenmeyer, *Hough-Transform and Extended RANSAC Algorithms for Automatic Detection of 3D Building Roof Planes from Lidar Data*. 2007.